Journal of Engineering Research and Reports

Volume 25, Issue 6, Page 153-165, 2023; Article no.JERR.102848
ISSN: 2582-2926

Optimal Configuration of Reactive Power in Distribution Network with Power Electronic Transformer

Can Zhang [a*] and Sixiang Ma [b]

[a] School of Electric Power Engineering, Nanjing Institute of Technology, Nanjing 211167, Jiangsu, China.
[b] CGN New Energy Nantong Co. Ltd., Nantong, Jiangsu, 210019, China.

Authors' contributions

This work was carried out in collaboration between both authors. Both authors read and approved the final manuscript.

Article Information

DOI: 10.9734/JERR/2023/v25i6931

Open Peer Review History:
This journal follows the Advanced Open Peer Review policy. Identity of the Reviewers, Editor(s) and additional Reviewers, peer review comments, different versions of the manuscript, comments of the editors, etc are available here: https://www.sdiarticle5.com/review-history/102848

Original Research Article

Received: 12/05/2023
Accepted: 14/07/2023
Published: 25/07/2023

ABSTRACT

Traditional means of reactive power regulation are limited to adjusting the ratio of the On-Load Tap Changer or changing the access position of the reactive power compensation device and its access capacity. In order to save the cost of putting in reactive power compensation devices, this paper proposes to use the characteristics of the reactive power output function on both sides of the power electronic transformer to regulate the system reactive power distribution. For this purpose, a reactive power optimization model including distributed power supplies and power electronic transformers is constructed with the objectives of minimizing voltage excursions, maximizing voltage stability margins and minimizing active losses in the network. At the same time, based on the characteristics of decision variables, cross-feedback hybrid optimization algorithm is used to solve different types of variables, and an improved wolf pack algorithm using Tent chaotic map and Levy flight strategy is proposed to improve the solution efficiency of the algorithm. The experimental results conclude that the proposed model and algorithm are valid, and the algorithm has significant advantages in terms of model solution time and global search capability when compared with the traditional Wolf Pack algorithms and Particle Swarm Optimization algorithms.

**Corresponding author: Email: zhangcan8211@163.com;*

Keywords: Reactive power optimization; improved wolf colony algorithm; power electronic transformer; voltage stability margin.

1. INTRODUCTION

With the development of the national economy, the improvement of user demand, and the development of large-scale new energy generation and high-penetration distributed renewable power all require the distribution network to be able to provide high-quality electric energy [1-3], for the distribution network The demand for better voltage control is becoming more and more urgent [4]. Reactive power and voltage control is the basis for ensuring the safe and stable operation of the power system. The study of reactive power optimization in the distribution network is of great importance for stabilizing node voltage, reducing line loss, improving power quality and transmission efficiency has practical significance, and is an important means to ensure the safe and stable operation of distribution network [5-7]. It is the most common adjustment method to adjust the reactive voltage of the distribution network through the on-load tap changer transformer (OLTC) and switching capacitors. This kind of method has low adjustment accuracy and slow speed, and is easily limited to the transformation ratio or changing the access position and access capacity of the reactive power compensation device. Although the static synchronous compensator has higher adjustment accuracy and faster speed, its cost is higher and it is difficult to meet the requirements of economical operation of the distribution network.

Power Electronic Transformer [8-11] (PET) is a transformer device that can provide high-quality electric energy, also known as Solid State Transformer (SST), Intelligent General Transformer (IGT), etc. PET can't only maintain the functions of traditional transformer power transfer and voltage conversion, but also better control the capacity and voltage of the primary and secondary sides, realize the flexible control and adjustment of the reactive voltage of the distribution network, and improve the voltage of the distribution network Stability [12] has received extensive attention in application fields such as smart distribution network and new energy Internet, and is the key equipment of the next generation smart grid [13-15]. Using PET as a reactive voltage adjustment method for reactive power optimization has obvious advantages over OLTC. Compared with traditional transformers, it is also more suitable for applications such as enriching system functions and improving system performance [8].

In recent years, there has been some research on reactive power optimization of distribution networks using PET at home and abroad. Literature [16] takes the voltage offset and network active power loss as the objective function, and uses the improved genetic algorithm to simulate the reactive power optimization method with power electronic transformer. The experiment shows that the application of power electronic transformer can optimize the reactive power of the power grid. Improve voltage quality and reduce reactive power loss. Literature [3] takes the active power loss and voltage offset of the system as the objective function, constructs the reactive power optimization model of the active distribution network including distributed power supply, energy storage components and PET, and uses the particle swarm algorithm to solve it. The experiment shows that, The effect of reactive power optimization using PET is better than OLTC. Literature [17] proposed a hybrid multi-objective optimization algorithm to solve the reactive power optimization model including PET, and the experimental results showed the feasibility of PET for reactive power optimization and the rapidity of algorithm solution. Literature [18] used PET for double-fed induction motor wind power generation system, and the experiment proved the effectiveness and superiority of PET for reactive power optimization.

The application of PET in the distribution network with distributed power can promote multi-energy complementarity in the region, realize efficient utilization and consumption of energy [19], and also have great advantages in voltage stabilization and reactive power compensation. However, the above documents all focus on proving the feasibility of PET applied to reactive power optimization of distribution network and the superiority compared with traditional transformers. There is a lack of research on solving the reactive power optimization model containing PET. Based on this, this paper regards PET as the core equipment of the active distribution network, combines wind power, photovoltaic and other distributed power sources with reactive power adjustment equipment, and established a multi-objective reactive power

optimization model with network loss, voltage quality and voltage stability as objective functions. And this paper proposed an improved wolf pack algorithm based on Tent mapping and Levy flight. According to different variable characteristics, the algorithm solves real variables and integer variables separately, and realizes the complete decoupling of variable ratio and capacity variables and solves the optimal transformation ratio and capacity to achieve the purpose of reactive power optimization. The simulation example analysis of the improved IEEE 33 node shows that the algorithm has good advantages in solving speed and global optimization ability. It is of great significance to save the cost of investing in reactive power compensation devices and to economically and stably operate the distribution network.

1.1 Reactive Power Optimization Model of Active Distribution Network with PET

1.1.1 The structure and principle of PET

A simplified model of PET is shown in Fig. 1:

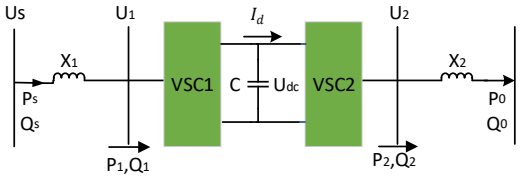

Fig. 1. PET simplified physical model

Among them, X_1 、 X_2 are DC side filter reactance; C is DC link capacitance; U_1、U_2 are voltage source converter (VSC) AC measured voltage amplitude respectively; U_S、U_0 are PET head end voltage amplitude respectively; P_s、Q_s are PET head end injection, P_0 、Q_0 are the active power and reactive power output by the terminal, respectively; P_1 、Q_1 are the active power and reactive power absorbed by the rectifier, respectively; P_2 、Q_2 are the active power and reactive power output by the inverter, respectively. According to the principle of PWM modulation [20], the reactive power mathematical model [21] can be obtained:

$$Q_S = U_S(U_S - M_1 U_{dc}/\sqrt{2}\cos\delta_1)/\mathrm{X}_1 \quad (1)$$

$$Q_0 = U_0(\mathrm{M}_2 U_{dc}\cos\delta_2/\sqrt{2}U_0)/\mathrm{X}_2 \quad (2)$$

Among them,M_1、M_2 are the modulation degrees of the primary and secondary sides of PET,δ_1、$\delta_2$are the modulation angles of the primary and secondary sides of PET. Considering the safety margin of the converter, there are δ_1<45° 、δ_2<45°, under this condition, Q_s、Q_0 respectively for M_1、M_2 to obtain the partial derivatives are: $\partial Q_s/\partial M_1<0$, $\partial Q_s/\partial M_1>0$, that is linear relationship with Q_s、M_1 , and Q_0、M_2. That is, the reactive power at the beginning and end of the PET can be controlled by M_1 and M_2.

$$\triangle Q_S = K_1 \triangle M_1 \quad (3)$$

$$\triangle Q_0 = K_2 \triangle M_2 \quad (4)$$

1.1.2 Objective function

In this paper, system network loss, voltage quality and voltage stability index (VSI) are used to judge the quality of distribution network status. The objective function is shown in formula (5):

$$y = \lambda_1 \frac{P_{loss}}{P_{loss0}} + \lambda_2 L_{\mathrm{ijmax}} + \lambda_3 \sum_{i=1}^{K} \frac{(\mathrm{U}_i - 1)^2}{U_{\max} - U_{\min}} \quad (5)$$

Among them, λ_1 、 λ_2 and λ_3 are weight coefficients, calculated by entropy weight method, and $\lambda_1+\lambda_2+\lambda_3=1$. $L_{ijmax} = \max_{l\in L}\{L_{ij}\}$, the expression of L_{ij} [7] is shown in formula (6). U_i 、 U_j are the voltage amplitudes of the first section and the end of the branch respectively; $\delta = \delta_i - \delta_j$; δ_i 、 δ_j are the voltage phase angles at the beginning and end of the branch respectively; K is the set of all branches in the distribution network; $U_{\max}$ 、 $U_{\min}$ are the voltage phase angles of all nodes in the distribution network Highest voltage and lowest voltage.

$$L_{ij} = \frac{4[(\mathrm{P}_i X_{ij} - Q_j R_{ij})^2 + (\mathrm{P}_j R_{ij} + Q_j X_{ij})U_i^2]}{U_i^4} \quad (6)$$

1.1.3 Constraints

Constraint conditions include power flow equation constraints, node voltage constraints,

branch current constraints and PET control variable constraints. The power flow equation constraints are:

$$\begin{cases} \sum_{i=1}^{N} P_i - P_L = U_i \sum_{i \in N} (\mathrm{G}_{ij} \cos\theta_{ij} + B_{ij} \sin\theta_{ij}) \\ \sum_{i=1}^{N} Q_i - Q_L = U_i \sum_{i \in N} U_j (\mathrm{G}_{ij} \sin\theta_{ij} + B_{ij} \cos\theta_{ij}) \end{cases} \quad (7)$$

In the formula: P_i、Q_i are the total active power emitted by DG; P_L is the active power absorbed by the load; B_{ij} is the imaginary part of the admittance between node i and node j; G_{ij} is the real part of the admittance between node i and node j. where the node voltage constraints are:

$$V_i^{\min} \le V_i \le V_i^{\max} \quad (8)$$

where, $V_i^{\max}$ and $V_i^{\min}$ are the maximum and minimum voltage amplitudes allowed by node respectively. The branch current constraints are:

$$|\mathrm{I}_{ij}| \le I_{ij}^{\max} \quad (9)$$

Where, $I_{ij}^{\max}$ is the maximum current that can flow through the branch between nodes i and j. Since different types of nodes have different power flow characteristics, different types of DG can't be connected to the same location. The PET control variable constraints are:

$$\begin{cases} P_{k1} = P_{k2} \\ \sqrt{P_{k1}^2 + Q_{k1}^2} \le S_k \\ \sqrt{P_{k2}^2 + Q_{k2}^2} \le S_k \end{cases} \quad (10)$$

Among them, P_{k1} and P_{k2} are the active power connected to the PET branch; Q_{k1} and Q_{k2} are the reactive power absorbed by the PET head and end. The reactive output constraints of photovoltaic and wind power are:

$$Q_{pvi,t}^{\min} \le Q_{pvi,t} \le Q_{pvi,t}^{\max} \quad (11)$$

$$Q_{pwi,t}^{\min} \le Q_{pwi,t} \le Q_{pwi,t}^{\max} \quad (12)$$

Among them, $Q_{pvi,t}^{\min}$ and $Q_{pvi,t}^{\max}$ are the minimum and maximum reactive power that can be compensated by the *i*-th photovoltaic power station at the moment *t*, respectively, and are the reactive power output by the *i*-th photovoltaic power station at the moment *t*; $Q_{pwi,t}^{\min}$ and $Q_{pw,i}^{\max}$ Are respectively the minimum and maximum reactive power that can be compensated by the *i*-th wind turbine at time *t*, respectively, $Q_{pwi,t}$ is the reactive power compensated by the first wind turbine at time *t*.

1.2 Model Solving Algorithm

1.2.1 Wolf pack algorithm

Wolf pack algorithm (WPA) [22] is a random probability search algorithm, which enables it to quickly find the optimal solution with a large probability. It can start searching from multiple positions at the same time, and between different search positions without interfering with each other. The wolves are mainly divided into alpha wolf, detective wolves and ferocious wolves. The alpha wolf is the most ferocious wolf in the wolf pack and is responsible for decision-making. Scout wolves are a relatively elite part of the wolf pack, they are responsible for wandering around looking for prey, and if they outperform the alpha wolf, they will replace them. The Detective Wolf communicates the location information of the prey to the head wolf, and the head wolf sends out a call, attracting the ferocious wolf to follow and keep looking for the optimal location. When the location of the head wolf is less than a certain distance, it will start to besiege the prey. This algorithm can be divided into the following steps:

1) Initialization. Set the number of wolves in the initial wolf pack to *N*, the dimension to *D*, the proportion factor of the detective wolves is *δ* the walking step is $step_s$, the running step is $step_b$, the siege step is $step_w$, the number of walking directions is *h* and the critical distance from running to siege is d_0.

2) Wandering behavior. In the solution space, the best S artificial wolves except the alpha wolf are regarded as the detective wolves,

and the prey fitness of each detective wolves is calculated respectively. If it is greater than the fitness of the alpha wolf, the detective wolf become the alpha wolf and re-initiate the calling behavior. Otherwise, the detective wolf will go further in the *h* direction according to the walking step:

$$x_{id}^{p} = x_{id} + \sin(2\pi p / h) \cdot step_{s}^{d} \tag{13}$$

Among them, *e* is the *P-th* direction, *i* is the *D-th* direction.

3) Summoning behavior. After the wandering behavior is over, an alpha wolf will be generated, and the alpha wolf will call the surrounding M ferocious wolves to the alpha wolf's position, and the ferocious wolves will quickly approach the alpha wolf with a running pace and search for prey. During the attacking process of the ferocious wolves, if the prey has a higher fitness, the ferocious wolf will replace the alpha wolf. When the distance between the ferocious wolf and the alpha wolf is less than the threshold, it will turn into a siege behavior.

$$x_{id}^{k+1} = x_{id}^{k} + step_{b}^{d} \cdot \frac{g_{d}^{k} - x_{id}^{k}}{| g_{d}^{k} - x_{id}^{k} |} \tag{14}$$

Among them, g_{d}^{k} is the current head wolf position.

4) Siege behavior. When the ferocious wolf senses the call of the alpha wolf, it immediately runs to the alpha wolf's position. During the running process, if it finds that the prey is more adaptable, it immediately replaces the original alpha wolf and directs other wolves to act.

$$x_{id}^{k+1} = x_{id}^{k} + \lambda \cdot step_{w}^{d} \cdot | g_{d}^{k} - x_{id}^{k} | \tag{15}$$

5) The number of iterations is increased by 1, and when the maximum number of iterations is met $T_{\max}$, jump to step 6), otherwise, substitute the detective wolves position at the front of the bulletin board and the randomly generated ferocious wolves position into step 2).

6) Output the optimal position and optimal fitness.

1.2.2 Feedback wolf pack algorithm

1.2.2.1Tent mapping and levy flight strategy

1) The algorithm proposed in this paper uses Tent mapping to initialize the population, and its mathematical expression is:

$$y_{m+1} = \begin{cases} \dfrac{y_m}{\alpha}, & 0 \le y_m < \alpha \\ \dfrac{1 - y_m}{1 - \alpha}, & \alpha \le y_m \le 1 \end{cases} \tag{16}$$

In the formula , $\alpha = 0.5$ Map the chaotic variables to the solution space of the problem to be solved:

$$Y = x_{\min} + (x_{\max} - x_{\min}) \cdot y \tag{17}$$

In the formula, $x_{\min}$ and $x_{\max}$ are the minimum and maximum values of variables, respectively.

2) Add the "Levy flight" search strategy to ensure that both near and far distances can be considered during the search process. The continuous jumping path and time *t* of Levy flight obey the Levy distribution, simplify and perform Fourier transform on it, and obtain the probability density function of its power form:

$$Levy \sim u = t^{-\lambda}, \ 1 \le \lambda \le 3 \tag{18}$$

In the formula, λ is the number of powers. The calculation formula for simulating the Levy flight path proposed by Mantegna is adopted:

$$l = u / | v |_{1/\beta} \tag{19}$$

$$\begin{cases} u - N(0, \sigma_u^2) \\ v \sim N(0, \sigma_v^2) \end{cases} \tag{20}$$

$$\begin{cases} \sigma_u = \left\{ \dfrac{\Gamma(1+\beta)\sin(\pi\beta/2)}{\Gamma[(1+\beta)/2]2^{(\beta-1)/2}\beta} \right. \\ \sigma_v = 1 \end{cases} \tag{21}$$

In the formula, l —Levy flight, β —parameter, take $0<\beta<2$; u、v —Normal distribution random number.

Introducing the random step size in Levy flight l makes the search direction and step size uncertain, so as to increase the diversity of population positions and improve the ability of the algorithm to jump out of local optimal solutions.

3) After joining the Levy flight strategy, the joiner performs position update according to formula (22).

$$X_{e,d}^{k+1}=\begin{cases} Q\cdot\exp\left(\dfrac{X_{worst}^{k}-X_{e,d}^{k+1}}{e^{2}}\right), & e>E_e/2 \\ X_{best}^{k+1}+l\cdot|X_{e,d}^{k}-X_{bset}^{k+1}|\cdot A^{+}\cdot W, & \text{else} \end{cases} \tag{22}$$

where: Q —Random numbers that follow a normal distribution; E_e —The size of the wolf group; W —A $1\times d$ matrix is all 1; $X_{e,d}^{k}$ —— The *d* dimension position of the *e*-th individual in the *k*-th generation; X_{best}^{k+1} and X_{worst}^{k} ——The optimal position occupied by the current discoverer and the current global worst position; A——a row of multidimensional matrix whose elements are 1 or-1 , and $A^{+}=A^{T}(AA^{T})^{-1}$.

1.2.2.2 Feedback wolf pack algorithm

In the comprehensive optimization model proposed in this paper, the number of variables contained is large and the types are different. Using the traditional wolf pack algorithm for optimization is easy to fall into a local optimum, and the same number of iterations is used for both variables, which is greatly improved. Increased the time used for optimization. In view of this, this paper proposes a Feedback Wolf Pack Algorithm (FWPA) with cross-feedback mechanism based on Tent chaotic map and Levy flight, and separate processing of EPT ratio variable X and reactive output variable Y. First, the reactive output variable Y is randomly generated, and the variable ratio variable X is optimized by using the wolf pack algorithm. After obtaining the optimized transformation ratio information X, then feed it back to the reactive output variable Y and optimize Y. Feedback the optimized reactive output variable Y to the transformation ratio variable X and optimize X. In this way, X and the Y are optimized repeatedly using the optimization information of the other party, and the number of iterations of the inner loop is separated. When the maximum number of iterations of the outer loop is met $T_{\max}$, the optimization process ends. The algorithm flow is as follows:

1) Initialization. Enter the node information, branch information and initial data of DG of the distribution network. Determine the number of wolves in the wolf pack is *N*, the dimension is *D*, the scale factor of detective wolves detection is *δ*, the walking step is $step_s$, the running step is $step_b$, the siege step is $step_w$, the number of walking directions is *h* and the critical distance from running to siege is d_0.
2) Optimize the individual variable ratio variable X. Initialize the individual reactive output variable Y, calculate the individual fitness, confirm the alpha wolf, and then perform behaviors such as wandering, calling, and besieging. After the position update is completed, the Levy flight mutation is performed on the selected individual. After iteration $t_{\max 1}$ times, the optimal individual position is output.
3) Optimize the reactive output variable Y. On the basis of determining variable ratio variable X, use wolf pack algorithm to optimize variable Y, the process is similar to step 2), and output optimal fitness and optimal position after iteration times.
4) Increase the number of iterations by 1, retain the fitness output of step 3), and compare it with the optimal fitness output of the previous step 3), if it is better than the previous optimal fitness, then retain the current position (X, Y), Update the optimal fitness for this iteration. When the maximum number of iterations is met $T_{\max}$, jump to step 5), otherwise, substitute the output optimal running variable Y into step 2).
5) Output the optimal solution and optimal position.

The algorithm flow of FWSA is shown in Fig. 2.

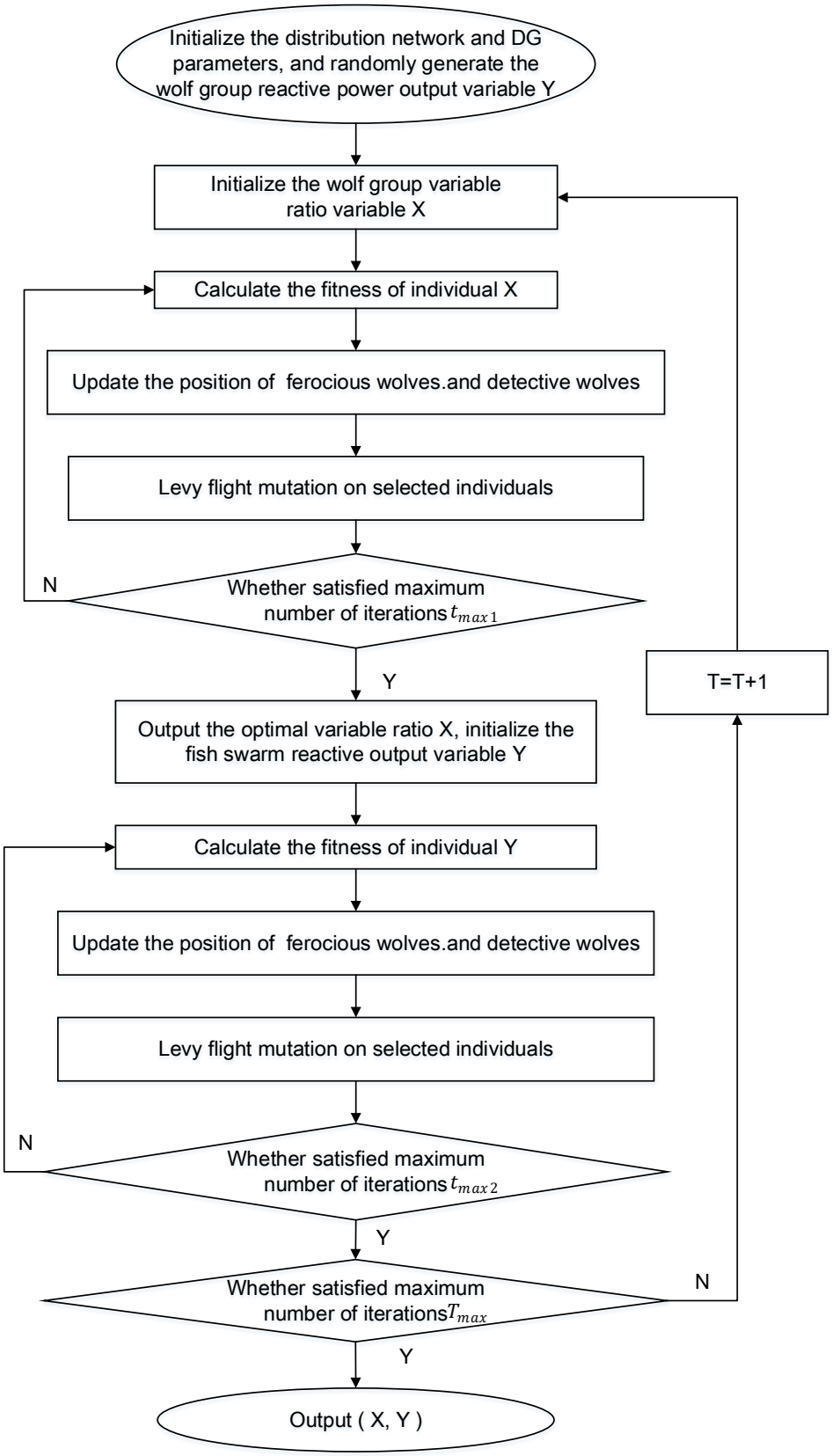

Fig. 2. FWSA algorithm flow

1.3. Case Analysis

1.3.1 Simulation parameters

In order to verify the superiority and effectiveness of the improved algorithm and reactive power optimization model established in this paper, as shown in Fig. 3, the improved IEEE 33 node power distribution system is analyzed. The system has a total of 33 nodes with a capacity of 10MW and a voltage level of 12.66kV. The load variation coefficient is shown in Fig. 4. Two wind power plants are connected to node 33 and node 22 respectively, with a capacity of 600kW; the photovoltaic power station is connected to node 18, with a rated power of 500kW; the power factor adjustment range of distributed power is -0.95~0.95; PET is connected to nodes 8 and 24 and 30. The number of wolves in the pack is 100, the scale factor of wolf detection is 0.5, and the number of walking directions is 20. The predicted value of wind power output is shown in Fig. 5.

1.3.2 Simulation calculation

In order to more fully illustrate the superiority of the improved wolf pack algorithm in the example environment, this paper compares the simulation effects of particle swarm algorithm (PSO), traditional wolf pack algorithm (WPA) and the proposed improved WPA algorithm. The fitness comparison curve is shown in Fig. 6.

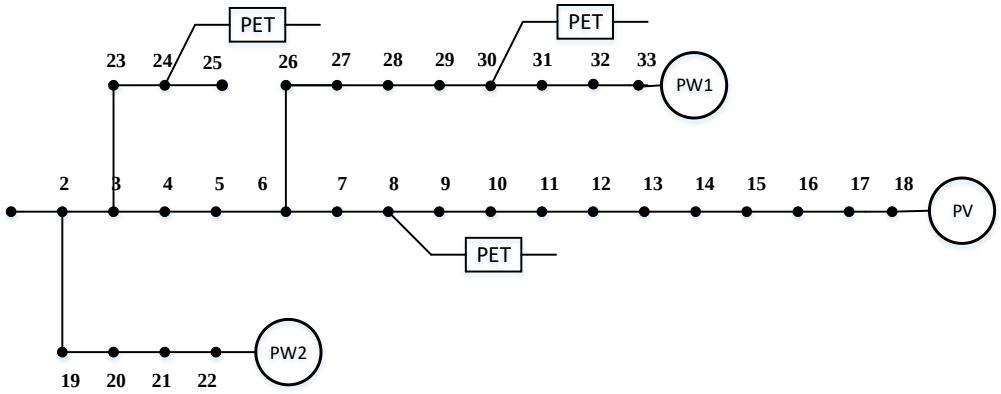

Fig. 3. Active distribution network with PET

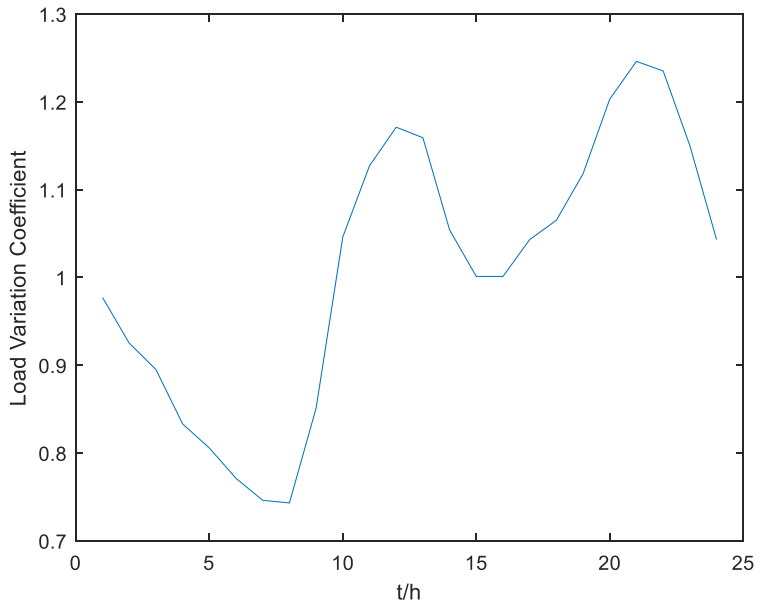

Fig. 4. Load variation coefficient

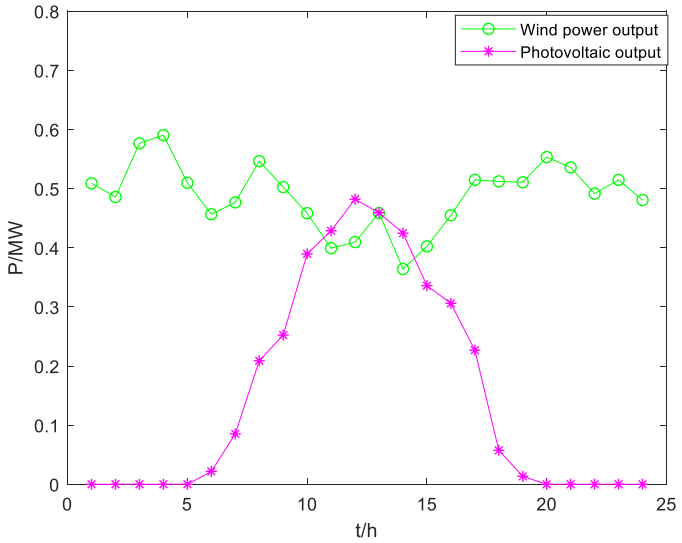

Fig. 5. Daily wind forecast output curve

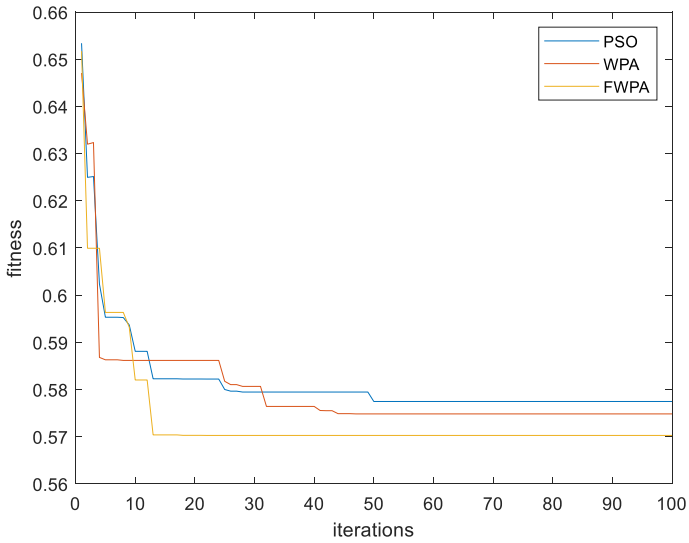

Fig. 6. Comparison of algorithm convergence

According to the comparison of the fitness curve in Fig. 6, it can be seen that the PSO algorithm starts to converge after 50 iterations, and the algorithm takes 42203s. The traditional WPA algorithm starts to converge after 44 iterations and takes 37501s. The improved WPA algorithm starts to converge after 12 iterations and takes 12618s. Obviously, the improved algorithm has a certain improvement in convergence and speed. The reason is that the FWSA algorithm splits complex variable combinations into two groups of variable combinations, which reduces the dimensionality of variable combinations and effectively improves the optimization speed. Secondly, although there are small loops nested in the large loop of the FWPA algorithm, the time of each iteration is longer than that of the WPA algorithm, but the reduction of the total number of iterations effectively reduces the time required for optimization.

According to the above mathematical model and algorithm application, the distribution network loss per hour of the three algorithms is output, and compared with the data before optimization. The comparison results of active network loss are shown in Fig. 7.

According to the comparison results in Fig. 7, it can be seen that during the peak period of power

consumption, that is, around 21:00 in the afternoon, the network loss of the distribution network can be as high as 252.71 kW when reactive power compensation equipment and corresponding optimization strategies are not used. After taking reactive power compensation measures, the active power loss of the system optimized by the FWPA algorithm can be reduced to about 150.51 kW. Within 24 hours a day, after the optimal configuration strategy of reactive power compensation equipment is completed through the FWPA algorithm, the maximum efficiency of system network loss optimization can reach about 53%, and the minimum value is about 40%. Combined with the above comparison results, the network loss of the distribution network system optimized by the FWPA algorithm is significantly reduced, and the optimized reactive power compensation equipment PET makes the power transmission efficiency of the distribution network significantly improved.

Select the moment of maximum load throughout the day to analyze the system voltage value, and output the node voltage before and after reactive power optimization at this moment. As shown in Fig. 8, the comparison results of the voltage change of the improved IEEE 33-node system including distributed power and PET are presented.

According to Fig. 8, it can be seen that when the system does not take reactive power adjustment measures, the system voltage reaches the lowest point of 0.93p.u. at node 32. When the PSO algorithm is used in it, the minimum amplitude of the node voltage is 0.95p.u., which appears at node 14. For traditional WPA optimization, the lowest node voltage value appears at node 14, which is about 0.95p.u. When the optimized FWPA algorithm is used, the lowest node voltage appears at node 14, reaching about 0.96p.u. In addition, the voltage value of node 32 at the lowest point of the original system voltage also increased to 0.96p.u., reaching the system voltage standard.

Further, analyze the voltage stability index comparison curve under the model in this paper, as shown in Fig. 9. Before optimization, the maximum value of the VSI index of the system is about 0.08 in the 22nd period; the minimum value appears in the 8th period, which is about 0.04. After the PSO algorithm and WPA algorithm are optimized, the peak-to-valley voltage VSI indicators are around 0.02 and 0.06 respectively. With the FWPA optimization strategy put into operation, the peak-to-valley VSI index is reduced to about 0.02 and 0.05. Compared with the traditional WPA algorithm and PSO algorithm, the VSI value optimized by the FWPA algorithm is lower at each moment, indicating that the improved optimization algorithm proposed in this paper has a stronger ability to improve system stability.

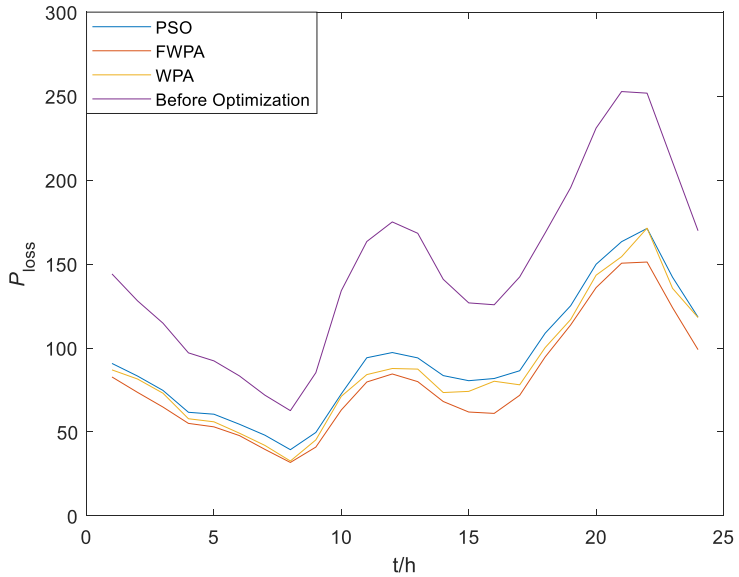

Fig. 7. System active network loss comparison

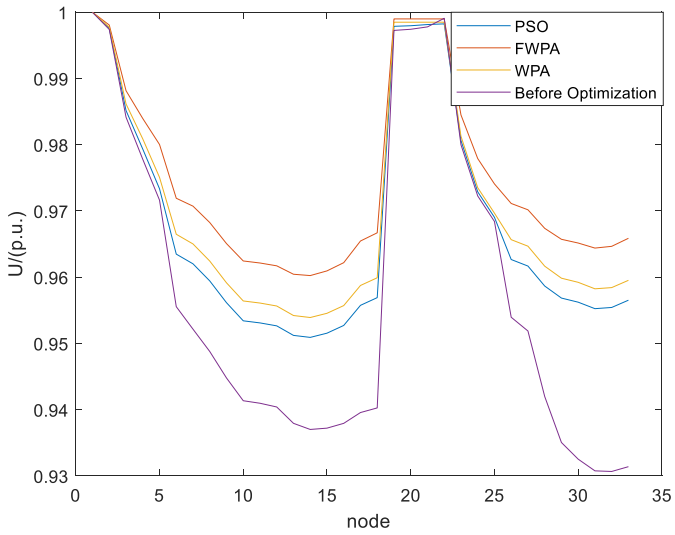

Fig. 8. IEEE 33 node voltage change curve and comparison

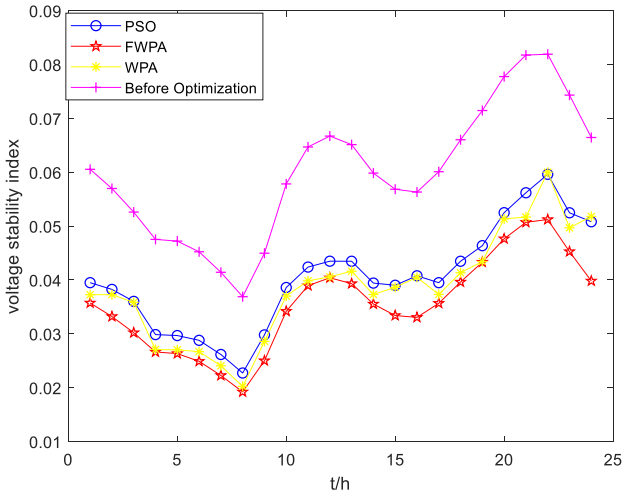

Fig. 9. Comparison curve of voltage stability index before and after optimization

2. CONCLUSION

This paper established a reactive power optimization model that comprehensively considers system active power loss, voltage quality and voltage stability margin, including PET, and proposed an improved wolf pack algorithm with cross-feedback mechanism based on Tent mapping and Levy flight to solve the problem according to the characteristics of different optimization variables. Through experimental analysis and comparison results, it can be seen that using the reactive power output capability of PET can effectively support the distribution network voltage, improve voltage, improve system stability, and reduce system active network loss. Compared with the traditional wolf pack reactive power optimization algorithm and particle swarm algorithm, the improved wolf pack algorithm can effectively improve the computing efficiency.

In this paper, wind power, photovoltaic and other distributed power sources are combined with reactive power adjustment equipment to participate in reactive power optimization simultaneously, which is of great significance to the safe and economical operation of the distribution network and the cost saving of investment in reactive power compensation devices. It provides a feasible solution for the stable operation of the distribution network after the new energy is connected to the grid. Combined with the reactive power compensation

capability of PET, the optimization of the energy structure is coordinated to improve the utilization rate of new energy such as wind power and photovoltaics in the distribution network. It provides reference and reference for reactive power optimization of distribution network system containing distributed renewable energy.

COMPETING INTERESTS

Authors have declared that no competing interests exist.

REFERENCES

1. Jiang Shan, Fan Chunju, Huang Ning, Zeng Jie. Fault characteristic analysis of DC pole-to-pole fault in power electronic transformer. Proceedings of the CSEE. 2018;38(5):1301-1309.
2. Li Zixin, Gao Fanqiang, Zhao Cong, Wang Zhe, Zhang Hang, Wang Ping, et al. Overview of power electronic transformer technology research[J]. China Electrical Engineering News, 2018;38(5):1274-1289.
3. Li Qi, Qiao Ying, Zhang Yujing. Continuous reactive power optimization of distribution network using deep reinforcement learning. Power System Technology. 2020; 44(4):1473-1480.
4. Zhang Xianglong, Zhou Hui, Xiao Zhihong, Zhang Wei, Wudi. Power electronic transformer applied to optimization of reactive powerin active distribution system. 2017;45(4):80-85.
5. Shu Xinlei, Gao Yang. Research on protection and self-healing control system of intelligent distribution network. Electrotechnical Application. 2021;40(11): 42-46.
6. Ding Tao, Liu Shiyu, Yuan Wei. A two stage robust reactive power optimization considering uncertain wind power integration in active distribution networks.IEEE Transactions on Sustainable Energy. 2016;7(1):301-311.
7. Hu Daner, Peng Yonggang, Wei Wei, Xiao Tingting, Cai Tiantian, Xi Wei. Multi-timescale deep reinforcement learning for reactive power optimization of distribution network. Proceedings of the CSEE. 2022;42(14):5034-5045.
8. Li Zixin, Gao Fanqiang, Zhao Cong, Wang Zhe, Zhang Hang, Wang Ping, Li Yaohua. Overview of power electronic transformer technology research. China Electrical Engineering News. 2018;38(5):1274-1289.
9. lu Ziguang, Zhao Gang, Yang Daliang, Zeng Xianjin. Overview of power electronic transformer technology in distribution network. Journal of Power System and Automation,.2016;28(5):48-54.
10. Ling Chen, Ge Baoming, Bi Daqiang. Research on power electronic transformers in distribution networks. Power System Protection and Control. 2012;40(2):34-39.
11. Zou Zhixiang, Buticchi G, Liserre M. Analysis and stabilization of a smart transformer-fed grid. IEEE Transactions on Industrial Electronics. 2018;65(2):1325-1335.
12. Li Sheng, Zhou Zhihao, Shan Qiqi, Jiani AN. Analysis of transient voltage stability in a low voltage distribution network using SST for the integration of distributed generations. Journal of Electrical and Computer Engineering. 2018;2018: 3498491.
13. Yuan Yubo, Shi Mingming, Shu Liangcai, HE Guohao, Chen Wu. Design method and experimental verification of power electronic transformer based on mixing modulation. Automation of Electric Power Systems. 2020;44(22):176-183.
14. Hu Liping, Sun Yingyun, Wang Chunfei, Pu Tianjiao, Chen Naishi, Sun Ke. Optimal combination of power electronic transformer operation strategy based on generalized sag control. Automation of Electric Power Systems. 2020;44(3):40-48.
15. Contreras JP, Ramirez JM. Multi-Fed power electronic transformer for use in modern distribution systems. IEEE Transactions on Smart Grid. 2014; 5(3):1532-1541.
16. Xie Daqin. Reactive power optimization control based on active distribution network voltage [J]. Electrical Application, 2015;34 (22):81-84.
17. Zhang Xiaoying, Hou Bingchen, Wang Kun, Chen Wei, Wang Xiaolan. Reactive power optimization of distribution network with solid state transformer based on improved beetle antennae search algorithm. High Voltage Apparatus.
18. Parseh N, Mohammadi M. Solid State Transformer(SST) interfaced Doubly Fed Induction Generator (DFIG) wind turbine. 2017 Iranian Conference on Electrical Engineering(ICEE). Tehran. 2017;1084-1089.
19. Falcones S, Ayyanar R, Mao X. A DC-DC multiport-converter-based solid-state transformer integrating distributed

generation and storage. IEEE Transactions on Power Electronics. 2013;28(5):2192-2203.
20. Tong Qian, Wu Wenjun, Ren Biying. Application of voltage source converter in power system. Beijing: Mechanical Industry Press; 2012.
21. Shi Jiying, Yang Wenjin, Xue Fei. Reactive power optimization of an active distribution network including a solid state transformer using a moth swarm algorithm. Journal of Renewable and Sustainable Energy. 2019;11(3):1-13.
22. Wu Husheng, Zhang Fengming, Wu Lushan. A new swarm intelligence algorithm-wolf pack algorithm. Systems engineering and electronic technology. 2013;35(11):2430-2438.

Peer-review history:
The peer review history for this paper can be accessed here:
https://www.sdiarticle5.com/review-history/102848